

Development of a Flush Air Data System for a Winged-body Re-entry vehicle

G. V. Rajesh Kumar* C. S. Harish* S Swaminathan[§] and Madan Lal**

*Scientist/Engineer [§]Group Director **Deputy Director

Launch Vehicle Design Entity, Vikram Sarabhai Space Center

Indian Space Research Organisation, Thumba, Trivandrum 695 022, India

Abstract

The paper addresses the development of a Flush Air Data System for a winged-body re-entry vehicle. An aerodynamic model and triples estimation algorithm from literature are adapted for this development. Numerical simulations are carried out using computational fluid dynamics codes for calibrating the model for Mach number range of 0.25 to 4.0. Effect of sensor measurement error on estimation algorithm is assessed using Monte Carlo simulations and expected errors are generated. Heat transfer analysis is carried out to arrive at an optimum length canalization system to maintain temperature at location of MEMS pressure transducer to 300 K. Frequency response analysis carried out to assess the sensor performance for the designed length of canalization indicates that the tube and sensor responses are acceptable up to 40 km of altitude.

Nomenclature

A, B	Angle of attack triples algorithm coefficients	α	Angle of attack, deg
A', B', C'	Angle of sideslip triples algorithm coefficients	α_e	Local angle of attack estimated by FADS, deg
A_c	Tube cross sectional area, m ²	β	Angle of sideslip, deg
c	Speed of sound, m/s	β_e	Local angle of sideslip estimated by FADS, deg
D	Canalization tube diameter, m	λ	Cone angle of FADS port, deg
f	Frequency, Hz	ϕ	Clock angle of FADS port, deg
L	Tube length, m	θ_i	Local flow incidence angle, deg
M	Estimation algorithm geometry matrix	μ	Dynamic viscosity, kg/m sec
M_∞	Free stream Mach number	ρ_0	Ambient density, kg/m ³
p	Port pressure, Pa	<u>Subscripts</u>	
p_∞	Free stream static pressure, Pa	i	Port index
q_c	Impact pressure, Pa	j	Iteration index
Q	Pressure weighting matrix		
R	Acoustic resistance		
V	Enclosed transducer volume		

1. Introduction

Successful mission management of a hypersonic re-entry vehicle requires knowledge of air data parameters like angle of attack, angle of sideslip, free-stream dynamic pressure, static pressure and Mach number. These air data parameters are required in real time with sufficient accuracy as they describe the state of the moving vehicle. These parameters find use in the flight control systems and autopilot system and facilitate improvement in accuracy of navigation systems and also assist in the overall mission management. These data are suitably interpreted during flight and the flight is manoeuvred in a profile, which limits the vehicle loads and thermal environment and also keeps the vehicle trajectory within the desired envelope.

Several types of air data systems like laser velocity meter systems, onboard Inertial Measurement Units (IMU) and intrusive boom type instruments like Pitot tube and mechanical vanes, available for measuring air data are addressed and reviewed in references.^{1,2,3,4} However, most of the above systems cannot be implemented for hypersonic vehicles because of the high energy nature of hypersonic flows. So, hypersonic flying vehicles essentially resort to the concept of flush air data system (FADS), wherein static pressures measured in a suitable matrix of pressure orifices located in and around the nose cone of the vehicle are used to compute the air data parameters.

This paper addresses the development of such an air data system required for the lifting re-entry vehicle.⁵ The paper is organized as follows: FADS overall system details are given in section 2. An estimation algorithm given in literature⁶ is adapted to estimate the air data states, and the details are described in section 3. Parameters required for calibration of the aerodynamic model are generated using numerical simulations and details are given in section 4. Effect of sensor errors on FADS algorithm are studied using Monte Carlo simulation and results are presented in section 5. Since, MEMS pressure transducers planned for flight have limitation on operating temperature, a suitable pneumatic tube length for FADS is arrived at by heat transfer analysis and the details are given in section 6. Frequency response studies of FADS canalization system with MEMS pressure transducer are studied and presented in section 7 with concluding remarks in section 8.

2. FADS: Details

FADS consist of a number of pressure tapping flushed with the vehicle surface, usually near the nose. The measured pressures at these ports are used to estimate air data. To perform this estimation, the air data states are related to surface pressures by an aerodynamic model⁶ given by

$$P_i = q_c [\cos^2 \theta_i + \varepsilon \sin^2 \theta_i] + P_\infty \quad (1)$$

where, θ_i the flow incidence angle is computed using

$$\cos \theta_i = \cos \alpha_e \cos \beta_e \cos \lambda_i + \sin \beta_e \sin \phi_i \sin \lambda_i + \sin \alpha_e \cos \beta_e \cos \phi_i \sin \lambda_i \quad (2)$$

A calibration parameter (ε) is introduced in the model to blend closed form potential flow solution for a blunt body,⁷ applicable at low subsonic speeds, and modified Newtonian flow model,⁸ applicable at hypersonic speeds.

Since the simple model of equation 1 is derived from potential and Newtonian flow around a blunt body, it is most valid near the vehicle stagnation point. Thus, the most desirable location for the FADS pressure matrix is close to the nosecap. A minimum of four pressure ports are needed to obtain a complete set of air data parameters, although more ports will increase the accuracy. But as reported in literature,⁹ improvements in accuracy start to decrease when more than nine ports are used. So, nine ports are selected for this vehicle for sufficient accuracy, of which five ports are arranged on vertical meridian in the plane of symmetry and other four ports along the fore-body as shown in **figure 1**. The port orientation is defined by cone angle (λ) and clock angle (ϕ) as given in **figure 1**. These angles for the nine ports are given in **table 1**. The cone angles for this vehicle are different from those reported in literature because of inclination of fore-body spherical cap with respect to the cone axis. Due to this, singularity checks required for computing side slip angle in the estimation algorithm, described in section 2 are more complex.

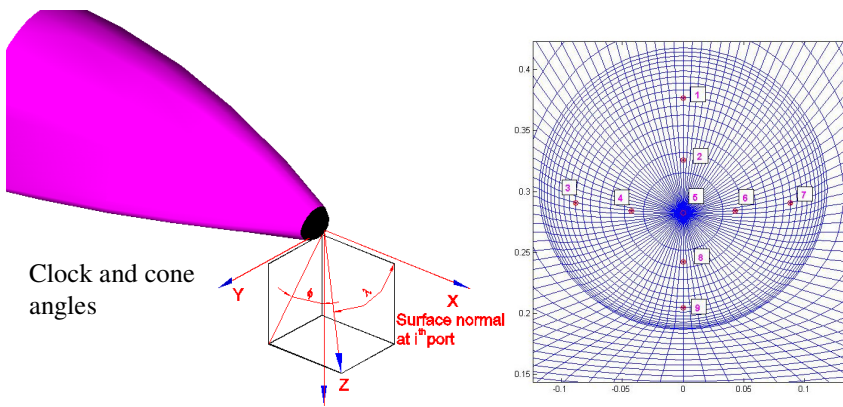


Figure 1: Pressure port arrangement with fore-body

Table 1: Cone and clock angles of FADS ports

Port Number	λ (deg)	ϕ (deg)
1	31.65	180
2	6.64	180
3	46.52	90
4	23.9	90
5	13.35	0
6	23.9	270
7	46.52	270
8	33.35	0
9	58.35	0

The schematic of FADS is shown in **figure 2**. Three MEMS pressure transducers in different pressure ranges of 20 kPa, 50 kPa and 120 kPa are connected to a single volume which communicates to the pneumatic plumbing. All the transducers have a proof pressure of 300 kPa. Depending on the range, appropriate transducer output which gives best accuracy will be selected by the onboard electronics and this pressure value will be used for onboard air data estimation. The signal-conditioned outputs of these pressure transducers are fed to the FADS processor in which the estimation algorithm is embedded. The FADS algorithm will be residing on an ADSP 21060 based system. This system is selected due to its advantages of reduced processing time for computation compared to conventional microprocessor or microcontroller based system¹⁰.

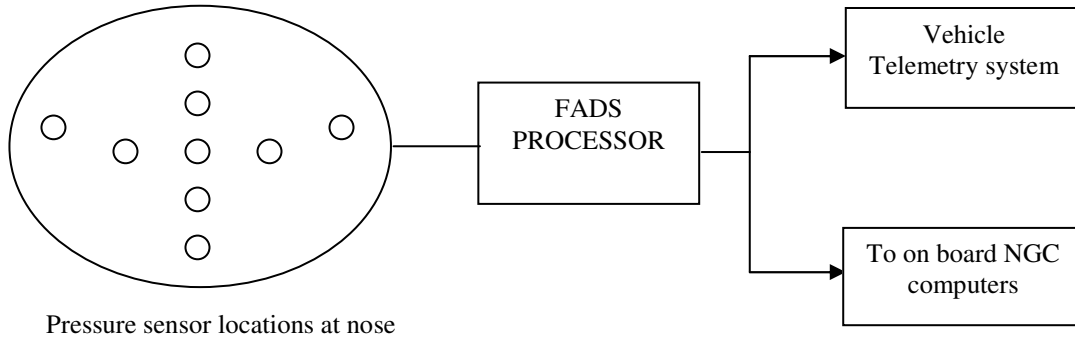


Figure 2: Schematic of FADS

The FADS processor output i.e., air data parameters are used by the onboard navigation, guidance and control (NGC) computer for the mission management of the vehicle. The air data parameters are also fed to the vehicle telemetry system for post flight evaluation.

3. FADS Estimation Algorithm

To estimate air data states from the aerodynamic model equations of 1 and 2, estimation algorithm developed by Whitmore et al called 'Triples algorithm'⁶ is used in the present study. This algorithm strategically takes three surface pressure ports (referred to as "triples") to compute the air data states. The five air data parameters are computed from the following equations⁶

$$\alpha_e = \frac{1}{2} \tan^{-1} \left(\frac{A}{B} \right) \quad (3)$$

$$A' \tan^2 \beta_e + 2B' \tan \beta_e + C' = 0 \quad (4)$$

$$\begin{bmatrix} q_c \\ p_{\infty} \end{bmatrix}_{(j+1)} = \left\{ \left[M^T_{(j)} Q M_{(j)} \right]^{-1} M^T_{(j)} Q \right\} \begin{bmatrix} p_1 \\ \vdots \\ p_n \end{bmatrix} \quad (5)$$

$$\frac{q_c}{p_{\infty}} = \left[1 + 0.2 M_{\infty}^2 \right]^{3.5} - 1 \quad \text{For subsonic flows} \quad (6)$$

$$\frac{q_c}{p_{\infty}} = \frac{166.92 M_{\infty}^7}{\left[7 M_{\infty}^2 - 1 \right]^{2.5}} - 1 \quad \text{For supersonic flows} \quad (7)$$

Port combinations available on the vertical plane are considered for angle of attack computations and other port combinations are used for side slip estimation. For the port arrangement shown in **figure 1**, there are 10 triple combinations available for angle of attack computation and 74 triple combinations for angle of sideslip estimation. Equation 4 used for sideslip estimation has two solutions. The proper choice of the root depends on which port arrangement is used to determine the angle of sideslip. Various port arrangements and resulting behaviour of the roots for all the 74 triples are examined and it is seen that 51 triples can be used for side slip estimation in the entire angle of attack range. The output angle of attack and sideslip are determined as the mean of the values computed using all the individual triples.

Three calibration parameters¹¹ viz., the calibration parameter (ϵ) given by equation 2, angle of attack correction ($\delta\alpha$) for correcting the estimated angle of attack obtained from equation 3 and angle of sideslip correction ($\delta\beta$) for correcting the estimated side slip angle obtained from equation 4 need to be evaluated for the FADS. These calibration parameters can be estimated either from flight experiments, ground based experiments, CFD, or analytical flow theory. Undoubtedly flight-generated correction factors are the most desirable. Correction factors may be obtained from ground based experiments, such as wind-tunnel tests, but these may not cover the entire flight envelope and are subject to the scale effects etc. Additionally, a large number of ground based experiments are needed, and performing them can be time-consuming and costly. But, using a validated CFD solver, correction factors can be generated and it is an attractive option due to its wide range of applicability and low cost. For the present studies, the calibration data are obtained from numerical simulations, the details of which are given in the next section.

4. Numerical Simulations and calibration parameters

Numerical simulations are carried out for the winged-body configuration to generate the necessary pressure data at the nine ports for different Mach numbers, angles of attack and sideslip. For subsonic flows, ($M = 0.25$ and 0.6) required pressure data at the nine ports are generated using panel methods. Complete vehicle is divided into 2790 panels for analyses. For supersonic flow, the flow field over the fore-body of the vehicle, where the pressure ports are arranged, is not affected much by the after body and hence the flow field analysis is carried out only for fore-body to reduce the computational time. Euler simulations are carried out using an in-house developed CFD code.¹² The code uses an automatic geometry adaptive three-dimensional cartesian grid system. It is a finite volume explicit solver. Explicit scheme is second order accurate in space and of TVD type which is achieved by means of min-mod type limiter. Inviscid fluxes are computed using approximate Riemann solvers.

Geometry is imported and cartesian grids are generated using inbuilt grid generator. Care is taken to ensure proper modelling and grid control parameters are selected so as to capture the body geometry completely. Appropriate boundary conditions are applied at the boundaries for subsonic and supersonic flows and tangency condition for velocity and adiabatic temperature are imposed on the walls.

Since flush air data algorithm solely depends on the accuracy of the computed pressure, solution is started with 1 million cells with refinement after every 4000 iterations. A grid of 5 million cells is used for the case of Mach number 3 after the final solution refinement. The final grid used for the solution is shown in **figure 3** along with a typical pressure coefficient flow field. The maximum pressure coefficient at the stagnation point is 1.75. Convergence is checked so that the value of $(P_{i+1} - P_i)/P_{i+1}$ is less than 10^{-5} between two iterations. Since the solver is based on explicit scheme, solution stability is ensured by taking CFL values less than 0.4. The solution has converged after 30000 iterations. The pressure data at the nine ports from these CFD simulations¹³ is used for generating the calibration parameters, the details of which are described here.

4.1 Estimation of calibration parameters

The FADS pressure model described by equations 1 and 2 has three parameters that must be determined by empirical calibrations viz., ϵ , $\delta\alpha$ and $\delta\beta$. Given a set of reference conditions (CFD/wind tunnel or flight data) that includes the surface pressure distribution, model parameters are estimated using the following equations¹⁰

$$\epsilon = \frac{\sum_{i=1}^9 \sin^2 \theta_i (C_{pi} - \cos^2 \theta_i)}{\sum_{i=1}^9 \sin^4 \theta_i} \quad (8)$$

$$\begin{aligned}\delta\alpha &= \alpha_e - \alpha \\ \delta\beta &= \beta_e - \beta\end{aligned}\quad (9)$$

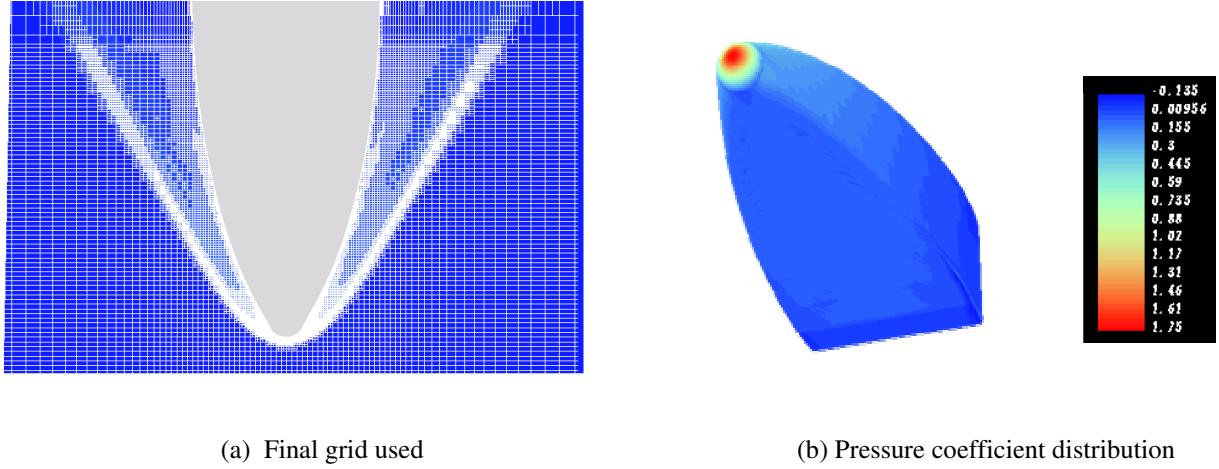


Figure 3: Grid and pressure coefficient distribution on fore-body for Mach number 3

Calibration parameter (ϵ):

The calibration parameter, ϵ , is generated for the re-entry vehicle using equation 8 for different Mach numbers at different angles of attack and sideslip. This data is curve fitted with second order polynomials in α_e and β_e , and the coefficients are scheduled as a function of Mach number. Equation 10 is the curve fit relation used and the coefficients of the equation generated for different Mach numbers are given in **table 2**

$$\epsilon = \epsilon_M [M_\infty] + \epsilon_{\alpha_1} [M_\infty] \alpha_e + \epsilon_{\alpha_2} [M_\infty] \alpha_e^2 + \epsilon_{\beta_1} [M_\infty] \beta_e + \epsilon_{\beta_2} [M_\infty] \beta_e^2 \quad (10)$$

Angle of attack and sideslip calibration:

Angle of attack calibration parameter ($\delta\alpha$) is evaluated for different Mach numbers at different angles of attack and sideslip using equation 9. These residuals are curve fitted with third order polynomials in α_e and β_e and the coefficients are scheduled as a function of M_∞ as given by equation 11. The coefficients of the equation for different Mach numbers are given in **table 3**

$$\begin{aligned}\delta\alpha &= A_0 [M_\infty] + A_1 [M_\infty] \alpha_e + A_2 [M_\infty] \alpha_e^2 + A_3 [M_\infty] \alpha_e^3 + A_4 [M_\infty] \beta_e + A_5 [M_\infty] \beta_e^2 \\ &+ A_6 [M_\infty] \beta_e^3 + A_7 [M_\infty] \alpha_e \beta_e\end{aligned}\quad (11)$$

Similar to angle of attack calibration, the angle of sideslip correction, $\delta\beta$, is generated and residuals are curve fitted with third order polynomial in α_e and β_e as given by equation 12. The coefficients of the curve fit generated for different Mach numbers are given in **table 4**

$$\begin{aligned}\delta\beta &= B_0 [M_\infty] + B_1 [M_\infty] \beta_e + B_2 [M_\infty] \beta_e^2 + B_3 [M_\infty] \beta_e^3 + B_4 [M_\infty] \alpha_e + B_5 [M_\infty] \alpha_e^2 \\ &+ B_6 [M_\infty] \alpha_e^3 + B_7 [M_\infty] \alpha_e \beta_e + B_8 [M_\infty] \alpha_e^2 \beta_e\end{aligned}\quad (12)$$

This software along with the calibration parameters is used to estimate the air data states for a typical trajectory point of $M_\infty = 2.5$, $\alpha = 20^\circ$, $\beta = 5^\circ$ and $P_\infty = 2000$ Pa. Pressure coefficient data at the nine ports are taken from CFD results. The results from the code are given in **table 5** along with the free-stream values and the comparison is good.

Table 2: ε curve fit coefficients for different Mach numbers

M:	0.25	0.6	1.5	2.0	3.0	4.0
ε_M	-1.044	-1.413	-9.79E-02	-5.55E-02	-0.105	-6.34E-02
$\varepsilon_{\alpha 1}$	-1.42E-03	1.40E-02	0.0063	2.99E-03	4.01E-03	1.34E-03
$\varepsilon_{\alpha 2}$	-6.34E-04	-9.82E-04	-2.10E-05	8.38E-05	5.30E-06	6.40E-05
$\varepsilon_{\beta 1}$	2.93E-02	9.63E-03	9.39E-03	-2.88E-04	-1.27E-03	2.27E-03
$\varepsilon_{\beta 2}$	1.02E-03	-4.69E-04	1.90E-03	2.16E-04	8.62E-04	3.29E-05

Table 3: $\delta\alpha$ curve fit coefficients for different Mach numbers

M:	0.25	0.6	1.5	2.0	3.0	4.0
A0	1.124	3.814	0.190	-0.357	0.823	-0.678
A1	-0.337	-1.201	-0.156	-0.133	-0.360	-8.16E-02
A2	5.56E-02	0.172	1.61E-02	1.60E-02	3.13E-02	1.07E-02
A3	-1.28E-03	-5.03E-03	-4.80E-04	-4.87E-04	-7.98E-04	-2.86E-04
A4	3.16E-02	-2.74E-02	-1.64E-02	8.61E-04	3.54E-02	0.104
A5	-1.82E-03	-7.81E-03	0	0	0	0
A6	0	0	0	0	0	0
A7	0	0	0	0	0	0

Table 4: $\delta\beta$ curve fit coefficients for different Mach numbers

M:	0.25	0.6	1.5	2.0	3.0	4.0
B0	0.845	2.023	-7.29E-02	-4.30E-02	-2.00E-02	-0.203
B1	-0.145	0.305	-7.32E-02	-0.122	-3.16E-02	-0.143
B2	2.77E-02	9.73E-02	0	1.23E-03	1.13E-02	0
B3	2.22E-03	4.63E-03	0	0	0	0
B4	-0.313	-0.372	-6.02E-02	1.50E-03	-4.74E-02	0.117
B5	3.24E-02	-3.04E-03	1.12E-02	1.46E-03	2.06E-03	-6.14E-03
B6	-1.15E-03	6.05E-04	-3.89E-04	-7.22E-05	-4.88E-05	3.22E-06
B7	0	0	0	0	0	0
B8	0	0	0	0	0	0

Table 5: Comparison of results from air data system software

Parameter	Free-stream	Results from FADS
P_∞ (Pa)	2000	2028.5
q_∞ (Pa)	8750	8700
Mach number	2.5	2.48
α (deg)	20	19.7
β (deg)	5	5.1

5. Effect of Sensor errors on FADS algorithm

Monte Carlo simulations are carried out for estimating the errors in calculation of angle of attack and angle of sideslip using the FADS algorithm due to errors in sensor pressure measurements. A Monte Carlo Simulation program is developed and analysis is carried out using this program. Initially, program calculates the angles of attack

and sideslip using the pressure values extracted from CFD code at the nine ports. Then, these pressure values at the nine ports are perturbed randomly within the sensor error limits and the new angle of attack and sideslip are computed. These simulations are continued till the convergence of the mean angle of attack is reached and the final results are presented.

Three pressure transducers in three different pressure ranges are planned to be used in the FADS. These pressure transducers have a $\pm 3\sigma$ error of 0.3% of Full Scale Reading (FSR). Transducer 1 will be used from 0 to 20 kPa range and will have a maximum error of ± 60 Pa. Transducers 2 and 3 will be used from 20 kPa to 50 kPa range and 50 kPa to 120 kPa range and will have maximum errors of ± 150 Pa and ± 250 Pa respectively. MC analysis is carried out at trajectory Mach numbers of 0.25, 1.5 and 4.0. These trajectory points cover the operating pressure ranges of the three transducers.

MC analysis is carried out for Mach number of 0.25 at 0.4 km altitude ($P_\infty = 90$ kPa) for 15° angle of attack and 0° angle of sideslip. Pressure values at the nine ports for this trajectory point are taken from CFD code. The pressures at the nine ports for this trajectory fall into the range of transducer 3. So, the pressures at the nine ports are perturbed randomly by ± 250 Pa at the nine ports. These perturbed values follow a normal distribution with mean zero and $\pm 3\sigma$ of 250 Pa. Number of simulations required for estimation is arrived at based on the convergence history of the angle of attack for all iterations. Analysis shows that 1000 simulations are sufficient to estimate the limits in the angle of attack and side slip computations. The mean and 3σ error in angle of attack and side slip for this case (A) are given in **table 6**. It is seen that the expected 3σ error in angle of attack and sideslip are 1.53° and 1.42° respectively.

MC analysis is carried out for Mach number 1.5 at 16 km altitude ($P_\infty = 11180$ Pa, $\alpha = 10^\circ$ and $\beta = -5^\circ$) and Mach number 4.0 at 33 km altitude ($P_\infty = 791$ Pa, $\alpha = 20^\circ$ and $\beta = -5^\circ$). The pressures at the nine ports for Mach numbers 1.5 and 4.0 fall into transducer 2 and 1 ranges respectively. Hence the pressures at the nine ports are perturbed randomly by ± 150 Pa and ± 60 Pa respectively with zero mean, as in the earlier case. The mean and 3σ errors in angle of attack and side slip for these cases are given in **table 6**. It is seen that the expected 3σ error in angle of attack and sideslip are 0.26 and 0.189 and 0.195 and 0.132 respectively for Mach numbers 1.5 and 4.0.

Table 6: MC simulation results for different trajectory conditions

Case	M	P_∞ (Pa)	P_{error} (Pa)	α			β		
				Nominal	Mean	3σ error	Nominal	Mean	3σ error
A	0.25	90000	250	15	15	1.53	0	0	1.42
B	1.5	11180	150	10	9.99	0.26	-5	-4.98	0.189
C	4.0	791	60	20	20	0.195	-5	-5.04	0.132

6. Heat transfer analysis of canalization system

MEMS pressure transducers planned for flight has an operating temperature limit of 300 K. The nose cap of the re-entry vehicle is a hot structure with inconel material. This structure will be exposed directly to the aerodynamic heating at re-entry and the temperatures are expected to go up to 1000 K.¹⁴ Since, the transducers have an operating limit of 300 K, they cannot be placed directly near the nose cap. So, suitable canalization for FADS has to be designed to limit the temperature to 300 K at the transducer location.

One dimensional transient heat transfer analysis is carried out and an inconel tube of 450 mm length followed by a PTFE rubber tube of 100 mm length is designed. Heat transfer by radiation from nose cap to the canalization system will be predominant. This radiation heat transfer from the nose cap is the driving parameter in estimating the temperature at the transducer location. Hence, thermal response of one canalization tube with nose cap is carried out using NISA heat transfer analysis tool¹⁵ to calculate the temperature at the transducer location.

Heat fluxes required for analysis are estimated using an in-house developed engineering code. Maximum heat flux at the stagnation point is 37 W/cm^2 . These heat fluxes are applied on the finite element model for analysis. The fore-body is assumed to be axi-symmetric about the nose cap axis and an axisymmetric analysis is carried out with 1700

finite elements. The finite element model with boundary conditions applied on the elements is shown in **figure 4**. Boundary conditions of convective heat flux and radiation to atmosphere are applied on the outer surfaces of nosecap and internal radiation is applied on the inner surfaces of nosecap, outer surfaces of canalization tube. Adiabatic wall condition is applied on remaining surfaces.

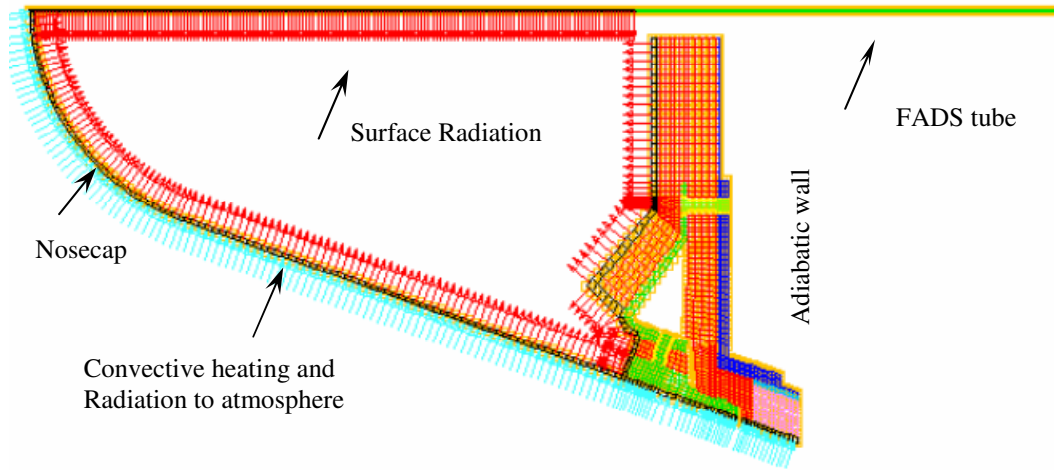


Figure 4: Finite element model of Canalization system with boundary conditions

Temperature histories along the length of the tube are shown in **figure 5**. The maximum temperature at the stagnation region is 1200 K and maximum temperatures at 100 mm, 200 mm and 300 mm length of inconel tube are 803 K, 717 K and 609 K respectively. The maximum temperatures at 350 mm, 400 mm, 450 mm (inconel tube end) and at the end of PTFE tube are 425 K, 336 K, 305 K and 300 K respectively. Analysis has shown that the material temperatures are within the design limits and canalization design can limit the temperature at transducer location (PTFE tube end) at 300 K. Based on this analysis, the length of tube is finalized as 550 mm.

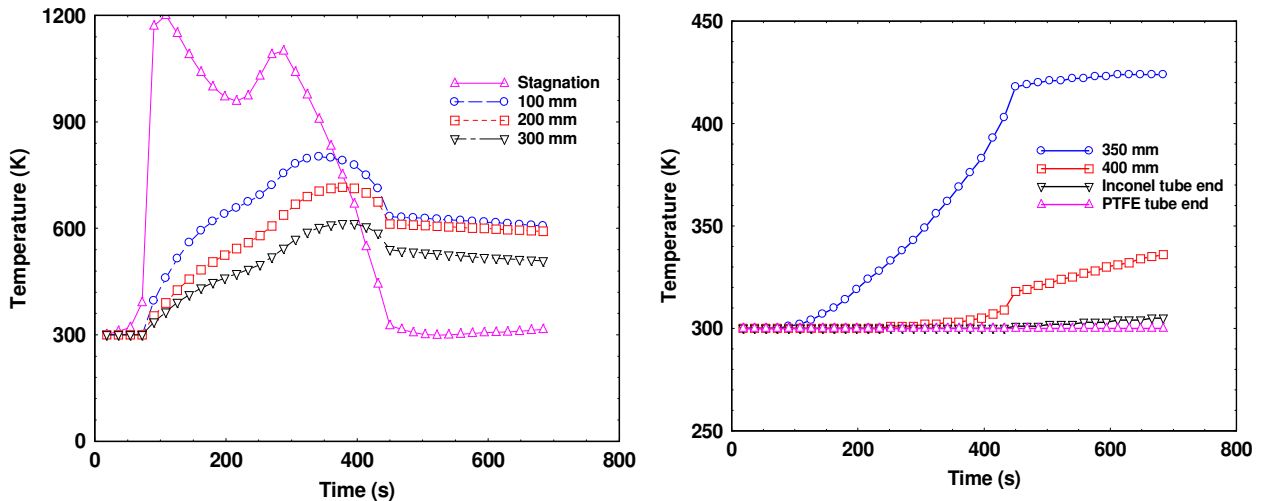


Figure 5: Temperature histories along the inconel canalization tube

7. Assessment of Sensor dynamics for the required length of tube

From heat transfer analysis, a tube of 550 mm length is arrived at for the FADS canalization system. MEMS pressure transducers will be placed at the end of this tube. In order to assess the response of transducer at the end of the tube, frequency response of FADS canalization system with MEMS based pressure transducers is carried out. The frequency response is estimated using equation 13 from reference¹⁶.

$$\frac{P_L(f)}{P_o(f)} = \frac{1}{\cosh[\sqrt{\alpha}L/c] + \frac{V\sqrt{\alpha}}{A_c c} \sinh[\sqrt{\alpha}L/c]} \quad (13)$$

Where $\alpha = -(4\pi^2 f^2) + j\left(2\pi \frac{R}{\rho_0} f\right)$
 $R = 32\mu/D^2$

Using the above equation, the frequency response is worked out for different altitudes using standard Indian atmospheric model and for tube length of 550 mm and tube diameter of 6 mm. The response curves for different altitudes are shown in **figure 6**. For higher altitudes, the available pressure will be less contributing to more phase lags as seen for 70 km altitude response. Response curves indicate that for the selected canalization tube length of 550 mm, the response of tube and sensor will be acceptable for altitudes up to 40 km.

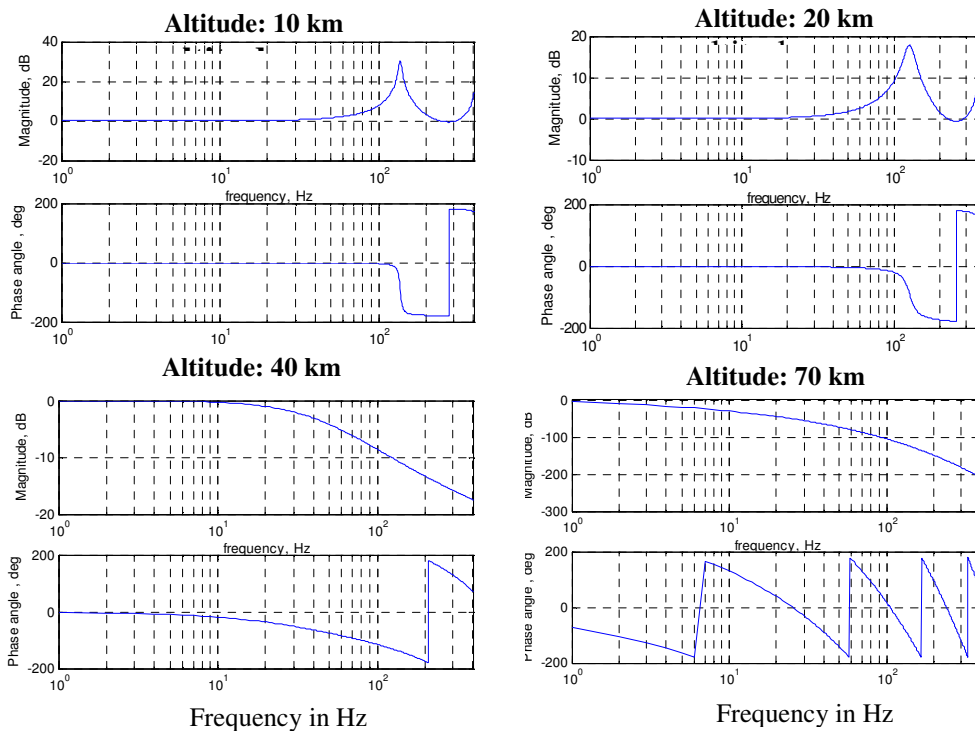


Figure 6: Magnitude and phase response for 550 mm tube length

8. Conclusions

Development of FADS for a wing-body configuration is discussed in detail. An aerodynamic model based on triples algorithm is adapted for application to non-axisymmetric fore-bodies. The aerodynamic model is calibrated using surface pressure data from numerical solutions, from panel code for subsonic flows and Euler code for transonic and supersonic Mach numbers. Curve fit coefficients for calibration parameters ϵ , $\delta\alpha$ and $\delta\beta$ are given. Effect of sensor errors on FADS algorithm is assessed. It is found that with sensor error of 0.3% of full scale reading, the error in α and β are about 1.5° for subsonic Mach number of 0.25. For supersonic Mach numbers of 1.5 and 4.0, these errors are less than 0.3° and 0.2° respectively. Heat transfer analysis of canalization system indicate a tube length of 550 mm. Frequency response analysis of the canalization system for different altitude condition indicate that the response of tube and sensor is acceptable for altitudes up to 40 km.

Acknowledgments

Authors wish to thank Dr. BN Suresh, Director, VSSC for his permission to publish this work. Thanks are due to Mr. Balram Panjwani for generating surface pressure data using computational fluid dynamics code. Authors acknowledge efforts of Mr. Yogesh S Parte in the initial stages of FADS development and Mr. T Sivamurugan in the thermal analysis. Authors also acknowledge Mr. Abhay Kumar for his review.

References

- [1] Benser, E. T., "Air Data Measurement for Hypersonic Vehicles," *SAE Technical Paper Series, Paper No. 912143*, Sep. 1991.
- [2] Ian Alexander Johnston, "Simulation of Flow Around Hypersonic Blunt-nosed Vehicles for the Calibration of Air Data Systems", Ph. D. Thesis, January 1999, The University of Queensland.
- [3] Gracey, W. H., "Measurement of Aircraft Speed and Altitude," NASA RP-1046, 1980.
- [4] Whitmore, S. A., Davis, R. J., and Fife, J. M., "In-Flight Demonstration of a Real-Time Flush Airdata Sensing (RT-FADS) System," NASA TM-104314, Oct. 1995.
- [5] Rajesh Kumar, G. V., Balram Panjwani and Sivamurugan, T., "Aero thermodynamic Analysis of Complete Windward surface of a Hypersonic Wing-Body Configuration Wing using Coupled CFD and Engineering methods" , *19th National Convention of Aerospace Engineers, "Indian Aerospace Engineering Perspective-2020"* , Nov 19-20, 2005, Jaipur.
- [6] Whitmore, Stephen A., Cobleigh Brent R., and Haering Edward A., Jr., "Design and Calibration of the X-33 Flush Airdata Sensing (FADS) System", NASA/TM-1998-206540, January 1998.
- [7] Currie, I. G., "Fundamental Mechanics of Fluid", McGraw-Hill Book Company, New York, 1974.
- [8] Anderson, John D., Jr., "Hypersonic and High Temperature Gas Dynamics", McGraw-Hill Book Company, New York, 1989.
- [9] Whitmore, S. A. and Moes, T. R., "Measurement Uncertainty and Feasibility Study of a Flush Airdata System for a Hypersonic Flight Experiment," NASA TM-4627, Jun.1994.
- [10] K C Finitha, G V Rajesh Kumar and et al, "Flush Air Data System Development", *Conference on Advances in Space Science and Technology (CASST'2007)*, January, 2007, Bangalore, India.
- [11] Cobleigh Brent R., Whitmore, Stephen A., and Haering Edward A., Jr., "Flush Airdata Sensing (FADS) System Calibration Procedures and Results for Blunt Forebodies", NASA/TP-1999-209012, Nov. 1999.
- [12] Balu, R. "Development of the Parallel Aerodynamics Simulator-3D (PARAS-3D) on a low-cost PC Cluster Platform", *Paper presented at the seminar on Parallel Processing, National Aerospace Laboratories, Bangalore, May 2000.*
- [13] G V Rajesh Kumar, Balram Panjwani and et al, "Calibration of Air Data Systems using Numerical Simulation of supersonic flow over Blunt fore-body", *20th National Convention of Aerospace Engineers*, Oct 29-30, 2006, Trivandrum, India.
- [14] T Sivamurugan, M M Patil and S Swaminathan, "Aerodynamic heating analysis of Reusable Launch Vehicle Technology Demonstrator", *54th AGM of Aeronautical society of India*, January 2003, Kolkata, India.
- [15] NISA II User's Manual
- [16] Stephen A. Whitmore and Timothy R. Moes -, "The effects of Pressure Sensor Acoustics on Air Data derived from High-Angle-of-Attack Flush Airdata sensing (HI-FADS) system", NASA Technical Memorandum 101736, February 1991.



This page has been purposely left blank